Original Article
Conventional MRI techniques combined with MR sialography on T2-3D-DRIVE in Sjögren syndrome

Yan-De Ren, Xiang-Rong Li, Jing Zhang, Li-Ling Long, Wei-Xiong Li, Yao-Qi Han

Department of Radiology, First Affiliated Hospital of Guangxi Medical University, Nanning, China

Abstract: Aim: To investigate the value of conventional MRI techniques combined with MR sialography on T2-3D-DRIVE in the diagnosis of Sjögren syndrome (SS). Methods: 107 patients were divided into SS group and non-SS group. Conventional MRI techniques, such as T1WI, T2WI, and STIR images were used for changes of fat signal in the parotid gland, while the MR sialography were used for ducts dilation of the parotid gland. Results: Among 93 SS patients, MRI identified abnormal fat deposit in the parotid glands in 86 patients. The fat signal based on MRI images showed 7 patients were in stage 0, 28 in stage 1, 14 in stage 2, 32 in stage 3 and 12 in stage 4. T2-3D-DRIVEMR MR sialography identified peripheral ducts dilation in 86 patients. The duct dilation based on MR sialography showed 7 patients in stage 0, 14 patients in stage 1, 44 patients in stage 2, 26 patients in stage 3, and 2 patients in stage 4. On MRI and MR sialography, both had a positive diagnostic rate of 92.5%. When MRI and MR sialography techniques were used together, the positive diagnostic rate increased to 96.8%. However, Kappa test showed that the MRI fat signal staging and MR sialogrpahy duct dilation staging had statistical difference (Kappa = 0.241, P = 0.000). Conclusion: T2-3D-DRIVE MR sialography detects peripheral ducts dilation in parotid glands with unmatched spatial resolution, also MRI fat suppression techniques detect diffusive fat deposit in parotid glands with high accuracy. Combining two techniques will provide optimal diagnosis workup for SS.

Keywords: Sjögren syndrome, salivary glands, magnetic resonance imaging, sialography

Introduction

Sjögren syndrome (SS) is an autoimmune disease characterized by lymphocytic infiltration in exocrine glands, such as the salivary and lacrimal glands, resulting in dry mouth and dry eyes. The diagnosis of Sjögren's syndrome involves clinical symptoms, serum tests for antibodies, radiological examinations and biopsy of the minor salivary gland. Commonly used imaging tests which will facilitate the diagnosis include X-ray sialography, salivary scintigraphy and various magnetic resonance imaging techniques (MRI). X-ray sialography is a sensitive and reliable method to detect the diffusive peripheral duct dilation, punctate sialectasis or contrast-filled peripheral cavities which are characteristic to SS with sensitivity and specificity of 79% and 95%, respectively [1]. However, X-ray sialography technique is invasive which requires manual skills for cannulation of the ducts, with a risk of radiation and iodine allergy. Salivary scintigraphy can measure the parenchymal and excretion function of all salivary glands simultaneously and quantitatively. It is easy to perform, reproducible and well-tolerated by the patient. However, it poses radiation exposure, and the uptake of 99mTc-pertechnetate may be affected by the thyroid function, which will in turn compromise the diagnostic accuracy and specificity [2].

Magnetic resonance imaging (MRI) is generally regarded as an important modality which allows a non-invasive evaluation of the complex anatomy of oral components of SS. Researchers have established MR imaging characteristics of the parotid gland in patients with SS, including high-intensity signal on T1-weighted MR images, which may indicate the presence of hemorrhages, proteinaceous content, or fat tissue [3], Fat-suppression MR techniques, such as STIR and fat saturation sequences, are able to detect premature fat deposition in the major salivary

glands in association with SS. Further study confirmed that the premature fat deposition was characteristic of SS, and the severity of fat deposition correlated well with the impaired rates of salivary flow in the SS patients [4]. Diffusion weighted imaging (DWI) is the only techniques available currently which allows mapping and measuring of the diffusion process of molecules, mainly water, in biological tissues and live organisms non-invasively. It has been increasingly used for parotid examination [5-8]. Using DWI, Regier et al [6] measured ADC values before and after acid stimulation in 52 healthy volunteers and 14 SS patients. The ADC values of the late stage SS patients were significantly lower than that of the healthy volunteers (P = 0.002) and early stage SS patients (P < 0.001). These MRI techniques, including T2-weighted imaging (T1WI), T1-weighted imaging (T2WI), and STIR, provide important information about parotid gland size/structural abnormalities, as well as fat deposit distribution and severity grading. It is a great supplementary tool to the gold-standard X-ray sialography [9-17].

MR sialography is based on the principle of MR hydrography in which stationary fluids are hyperintense on heavily T2 weighted images. This technique is noninvasive with rapid acquisition of images that demonstrate the main duct and intraglandular branches up to second order branching in the salivary glands. MR sialography can visualize parotid ducts wall damage and abnormality in the gland parenchyma [14]. In addition, MR sialography is less bias when examine the duct system; and it allows delayed observation of the ducts system [18]. Various MRI techniques have been used in clinic for MR sialography, e.g., 3D T2-WI with thin slice and high resolution using a fast-spin echo sequence with a flip-back driven equilibrium pulse (T2-3D-DRIVE), fast imaging with steady state precession (FISP), fast imaging with steady state acquisition (FIESTA), 3D constructive interference in steady state (3DCISS), and half fourier acquisition single-shot turbo spin-echo (HASTE) sequences, etc. In present study, we used T2-3D-DRIVE embedded in 3.0T MR scanners by Philips, combined with T1, T2, and STIR MRI scans, to characterize the parotid gland in SS patients and evaluated the diagnostic value of different MRI techniques.

Materials and methods

This study was performed in accordance with the criteria of the Helsinki Declaration and was approved by the Institutional Review Board of our institute. All subjects signed informed consents to participate in the study.

Patients

Between November 2012 and December 2013, 107 patients in The First Affiliated Hospital of Guangxi Medical University suspected of having SS because of xerostomia were enrolled. All patients were over 18 years old, had chronic symptoms of xerostomia and recurrent parotid gland swelling. Patients with tumors of the salivary glands and/or head/neck radiation therapy history were excluded. Based on the diagnostic criteria of SS proposed by the American-European Consensus Group [19], patients were divided into SS group (n = 93) and non-SS group (n = 14). Two groups of patients are excepted for the following situation, history of neck and craniofacial radiation therapy, hepatitis virus C infection, AIDS, lymphoma, nodules disease, graft versus host disease, resist acetyl choline medicine application (e.g, atropine, scopolamine, propantheline bromide, belladonna, etc). In the 93 SS patients, there were 71 females and 22 males, with an average age of 46 ± 9 years old (range 18-75 years) and the disease course ranged from 3 month to 7 years. In the 14 non-SS patients, there were 11 females and 3 male, with an average age of 47 ± 7 years old (range 23-68 years) and disease course ranged from 1 month to 12 years. In the 20 healthy volunteers, there were 17 females and 3 males, with an average age of 43 ± 6 years old (range 18-65 years).

MRI scans

MRI of the parotid glands was carried out with a 3.0T MR imager (Achieva 3.0T, Philips). One hour prior to the scheduled scan time, the patients were asked to do not eat or drink. During the scan, the patients lay on supine position to ensure laterally symmetrical and were instructed to avoid swallowing. The MR images were obtained with spin-echo sequences as follows: T1-weighted, TR/TE = 550 ms/10 ms; T2-weighted, TR/TE = 2600 ms/80 ms; SITR: TR/TE = 1000 ms/80 ms, TI = 120 ms. Both axial and coronal scans were obtained on

all subjects with a slice thickness of 3 mm for T1WI, T2WI and STIR. For MR sialography, imaging parameters for the T2W-3D-DRIVE sequence were as follows: TR/TE = 2000 ms/200 ms, slice thickness = 0.5 mm. The oblique sagittal image plane necessary to cover the whole course of the parotid gland main duct was used since the duct has a small C-shaped curve anteriorly as it bends around the masseter muscle.

Image analysis

The MR images were analyzed by two radiologists specialized in the head and neck on MR images. The two radiologists did not know any other clinical information about these patients. The radiologists evaluated the signal intensity of both parotid glands on MR images and the presence/absence of peripheral duct dilation in parotid glands on MR Sialography. T1WI, T2WI, and STIR images were used for fat signal staging. MR sialography was used for ducts dilation staging. The diagnostic values of MRI and MR sialography for SS were compared. Since SS involves bilateral parotids glands, the analysis was focused on left parotid gland only. Fat signal staging and duct dilation staging were evaluated individually and independently. Disagreements were resolved through discussion until consensus was reached.

High-intensity areas on T1-weighted images of the parotid glands in SS patients are due to increasing fat deposition in the glands. Typically, the appearance of high-intensity areas on T1-weighted MR images of the parotid gland implied the presence of fat tissues. The STIR sequence converted the parotid gland to a high-intensity-rich organ with multiple spots of low or no signal intensity, which corresponded to the high-intensity spots on T1WI. Based on the characteristic appearances of fat signal on T1WI, T2WI, and STIR images, as well as grading methods reported by Izumi and Regier's [3, 4], our modified grading system was as follows: grade 0, homogeneous intensity distribution, no abnormal fat signals detected, normal parotid glands; grade 1, sparse distribution of streaks-like fat signals; grade 2, diffusive distributed, honeycomb-like fat signals; stage 3, diffusive patchy fat signal, less than 50% of total area of whole parotid glands, nodular appearance of residual glands; stage 4: mas-

sive homogeneously distributed fat signal on T1-weighted images, more than 50% of whole parotid glands, barely see any normal gland structure.

The MR sialographic stages of SS were determined according to the criteria proposed by Tonami et al [11, 13], in which stage 0 = normal. Stage 1 = punctate, in which diffuse, spherical areas of high-signal intensity, 1 mm or less in diameter and uniform in size, are distributed evenly throughout the gland. Stage 2 = globular: in this stage of disease, the spherical areas of high signal intensity increase to 1 to 2 mm in diameter. Stage 3 = cavity: with further disease progression, the areas of high intensity coalesce and enlarge further, more than 2 mm in diameter. Stage 4 = destructive, in which there is marked dilation of the main duct with an irregular diameter, as well as irregular branching.

The usefulness of MRI and MR sialography in diagnosis of SS

Based on American-European Consensus Criteria for SS, the definite SS diagnoses were made when fat signal grade > 0 and MR sialography grade > 0. Using these diagnosis criteria, the diagnostic value of MRI, MR sialography and combination of two techniques were compared.

Statistical analysis

The data analysis was performed using SPSS17.0 software. The difference between MRI imaging and MR sialography for SS diagnosis was compared using χ^2 test. Kappa test was used to analyze the consistency between MRI fat signal staging and MR sialogrpahy duct dilation staging. Kappa value no less than 0.75 indicated highly consistent; kappa value between 0.40 and 0.75 indicated moderate consistent; and Kappa value less than 0.40 indicate inconsistent. The *P* value less than 0.05 was considered statistically significant.

Results

MR imaging and grading of SS

Of 93 SS patients, eighty-six patients had heterogeneous MR signals with different degree of fat signals. In the early stage of disease, T1WI
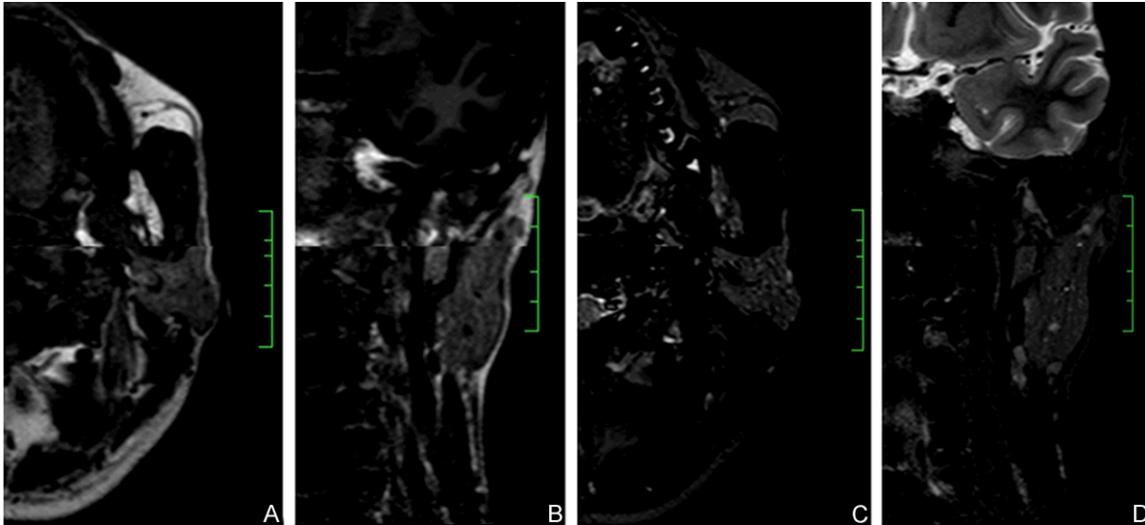
Figure 1. Fat signal grading's on MRI images. Images were from same patient with Sjögren syndrome, fat signal grade 2. (A and B) were representative axial and coronal MR images showing heterogeneous signal distribution within parotid gland, with diffusive honeycomb-like fat signals which intensity was comparable with subcutaneous fat tissue. (C and D) were axial and coronal STIR images. The high-intensity signals observed on the T1-weighted images of the parotid glands were converted into decreased signal at corresponding areas. Some sporadic high-intensity signals indicated dilated peripheral ducts.

showed multiple high-intensity streaks-like signals and T2WI may have normal appearance. As the disease progressing, T1WI and T2WI images showed honeycomb-like, patchy, or diffusive high intensity areas, while SITR images had low intensity or no signal at the areas corresponded to the high-intensity areas on the T1-weighted images (**Figure 1**). Based on the fat signal intensity, the 93 SS patients were graded as grade 0 (n = 7), grade 1 (n = 28), grade 2 (n = 14), grade 3 (n = 32) and grade 4 (n = 12). Among the 86 SS patients, number of patients at stage 3 was highest, followed by that of stage 1.

Characteristic patterns and grading of SS by MR sialography

Among 93 SS patients, eighty-six patients had peripheral ducts dilation, which was observed in both parotid glands. On the sialographic images, the dilation was presented as diffusive spherical, globular, or cavities like high-intensity area; two patients, the main duct became stiff, had focal enlargement, and showed sausage-like or beaded like lesions; and five patients did not have abnormal changes on MR sialography (**Figure 2**). Based on the dilation of duct, the 93 SS patients were graded as grade

0 (n = 7), grade 1 (n = 14), grade 2 (n = 44), grade 3 (n = 26) and grade 4 (n = 2). Among which, the number of patients at stage 2 was the highest.

Comparison of diagnostic value of MR imaging and MR sialography

In 20 healthy control and 14 non-SS patients, no abnormal fat signals were observed on T1WI, T2WI, and STIR images; and no duct dilation was observed on MR sialography. No false positive was observed.

In 93 SS patients, both MR imaging and MR sialography detected 86 SS patients (92.5%). No false positive was observed. Two imaging modalities showed comparable diagnostic sensitivity for SS. When two imaging modalities, MR imaging and MR sialography, were used together, ninety out of 93 SS patients were diagnosed. The diagnostic sensitivity improved to 96.8%. Two grading systems (MR imaging and MR sialography) were consistent regarding the diagnostic sensitivity of SS (P < 0.01); however, there was disagreement on SS grading between MR imaging fat signal intensity and MR sialography duct system dilation evaluation (**Figure 3**); the kappa value less than 0.4 (**Table 1**).
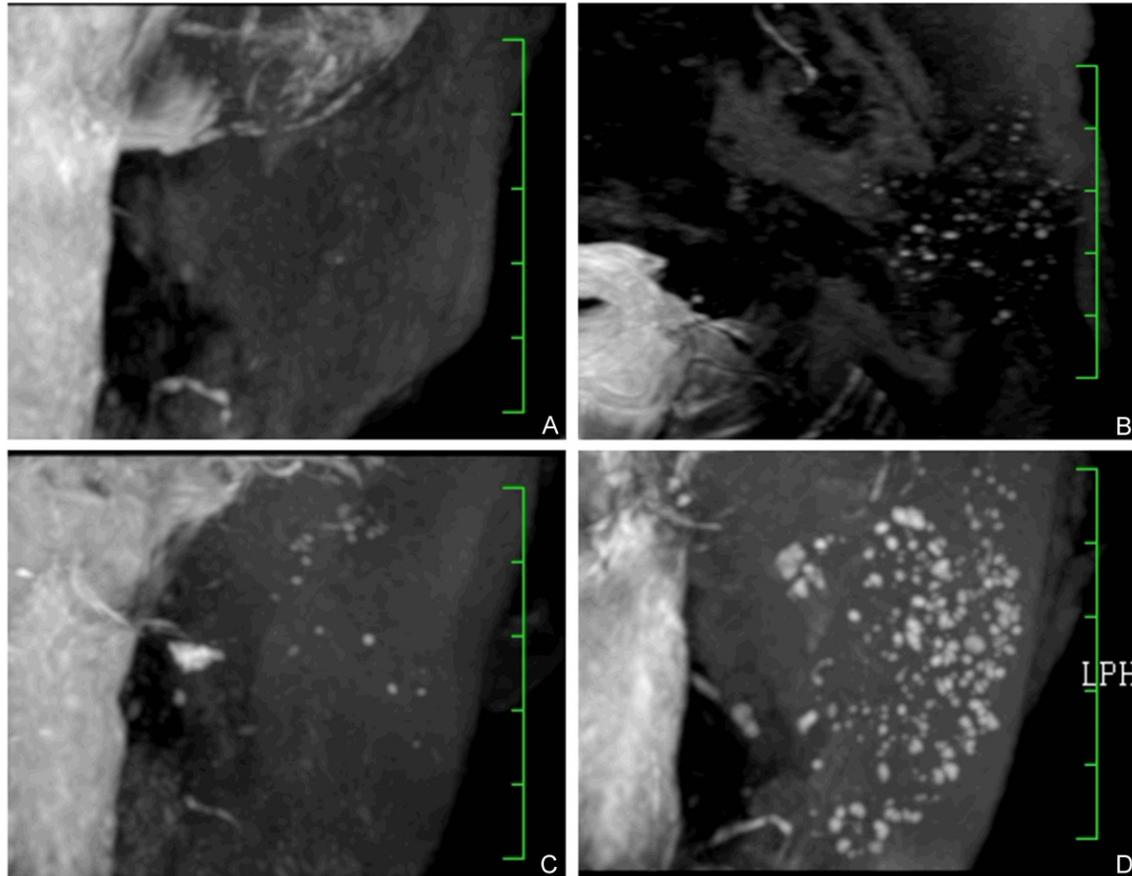
Figure 2. 3D-T2-DRIVE MR sialography grading. Images showed grade 1 to 4 duct dilation. A: Grade 1, punctate areas of high-signal intensity, 1 mm or less in diameter. B: Grade 2, globular spherical areas of high signal intensity, 1 to 2 mm in diameter. C: Grade 3, cavity-like areas of high intensity coalesce and enlarge further, more than 2 mm in diameter. D: Grade 4, marked dilation of the main duct with an irregular diameter, as well as irregular branching.

Discussion

Usefulness of routine MRI imaging in the diagnosis of SS

In SS, there is massive lipid infiltration and degeneration in parotid glands. In the early stage of fat infiltration, sparse punctate or streaks-like high signal spots are commonly observed on T1WI images, while the signal change on T2WI and STIR is not obvious. With advancement in the severity of disease, the fat deposition progresses, as evidenced by diffusive high-signals with stripe-, lattice-, or patchy-appearance on T1WI and T2WI. However, regardless of grading, the distribution of fat signal is diffusive and irregular, which is characteristic for parotid glands in SS patients [4, 13]. In our opinion, T1-weighted imaging is more sensitive to the fat signal change and therefore more valuable than T2-weighted imaging and STIR.

However, the STIR sequence converted the high-intensity signal on the T1-weighted images of the parotid glands into decreased signal at corresponding areas. When two MR techniques are used collaboratively, the fat signal distribution and characterization, as well as fat signal grading, will be more accurate [13].

It's been reported that MR imaging provides diagnostic sensitivity and specificity for SS of 71%~100% and 93-100%, respectively [10, 11, 14-16]. In present study, the MR imaging gave diagnostic sensitivity and specificity of 92.5% and 100% (no false positive), respectively, which were consistent with literature report. Our results demonstrated that MR imaging is a well-recognized, facile yet effective tool for SS diagnosis and it can be widely used to detect the parotid gland abnormality and to differentiate SS from other parotid diseases.
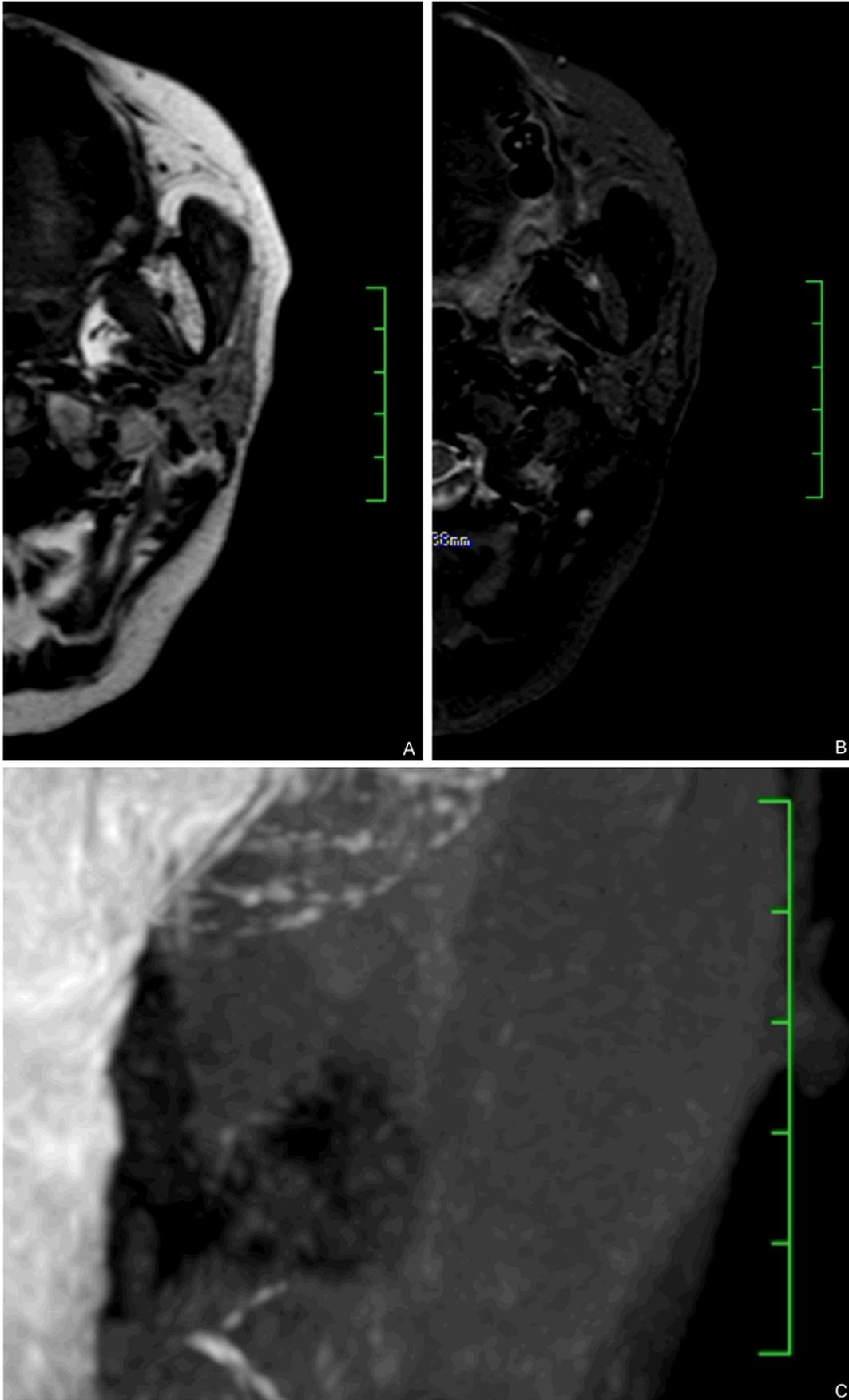
Figure 3. Combination of MRI imaging and 3D-T2- DRIVE MR sialography identified unparalleled fat deposition and ducts dilation. (A and B) showed axial T1WI and STIR showing diffusive fat signal, more than 50% of whole parotid glands, barely see any normal gland structure. The results indicated this patient is fat signal grade 4. However, in the same patient, MR sialography image (C) showed moderate grade 2 peripheral duct dilation.

Table 1. The consistency of fat signal grading and parotid ducts dilation grading in 93 patients with Sjogren's syndrome (P = 0.000, Kappa = 0.241)

Fat signal grading	Ducts dilation grading					Total
	Grade 0	Grade 1	Grade 2	Grade 3	Grade 4	
Grade 0	3	4	0	0	0	7
Grade 1	2	6	17	3	0	28
Grade 2	0	0	10	4	0	14
Grade 3	0	4	7	19	2	32
Grade 4	2	0	10	0	0	12
Total	7	14	44	26	2	93

Usefulness of MR sialography in diagnosis of SS

Lomas et al first reported a magnetic resonance (MR) imaging protocol that uses a heavily T2-weighted (echo time, 750 ms), fat-suppressed pulse sequence and rapid acquisition with relaxation enhancement [20]. This MR technique can successfully demonstrate both normal and abnormal parotid and submandibular gland duct systems; it has been increasingly used in clinical and improved over time (e.g. T2W-3D-DRIVE sequence was embedded in commercial MRI scanners). T2W-3D-DRIVE is based on 3D turbo spin-echo (TSE) sequence with a set of recovery pulses applied at the end of the echo train to push the residual transverse magnetization back to the longitudinal axis. The contrast achieved with TSE and DRIVE provides heavily T2-weighted MR images of higher image quality, less susceptibility artifacts and brighter fluid signals. The addition of the DRIVE pulse to the T2-weighted 3D TSE sequence is preferable when imaging the cranial nerves surrounded by the cerebral spinal fluid, or fluid filled structures because of shorter scan time and better imaging quality due to reduced flow artifacts. It has been widely used for inner ear imaging [21]. However, the application of DRIVE sequence has not been reported for parotid gland ducts imaging. In present study, we used DRIVE sequence for parotid gland duct imaging. Our data indicated that T2W-3D-DRIVE sequence provides higher signal to noise ratio, contrast to noise ratio, and spatial resolution; it can clear visualize the dilated peripheral parotid gland ducts with sharp edges. After MIP image reconstruction, dilated ducts can be clearly distinguished from the surrounding parotid parenchyma with lower signal intensity. The excellent contrast between ducts and parenchyma readily meets the requirements for peripheral ducts imaging.

The technique presented here has the positive rate of 92.5% and specificity of 100% for detection of peripheral ducts dilation; it can also grade the severity of duct dilation. Gadaodia [14] compared two other 3D MR sialography techniques, 3D-CISS and HASTE, for the detection of duct dilation in patients with chronic parotitis. The results showed that the diagnostic sensitivity and specificity were 100% and 87% for HASTE, 90% and 75% for 3D-CISS, respectively. When two techniques were combined, the diagnostic sensitivity and specificity were 93% and 100%, respectively. We can see that T2W-3D-DRIVE is comparable with 3D-CISS and HASTE regarding diagnostic sensitivity and specificity; it's a facile and valuable tool for diagnosis of parotid duct dilation.

The usefulness of combining MR imaging and MR sialography in diagnosis of SS

When the commonly used MRI sequences such as T1WI, T2WI and STIR are combined with 3D-DRIVE technique, it provides diagnostic sensitivity and specificity of 96.8% and 100%, respectively. This result demonstrated that combination of these techniques could improve the diagnostic sensitivity for SS, which is consistent with literature report [9, 22, 23].

The SS patients also had characteristic fat signal patterns. In our study, most of the SS patients had stage 3 fat signal abnormalities, followed by stage 1. Therefore, we propose that the patchy- or streak-like fat signal abnormality is more frequently observed in patients with SS. Meanwhile, forty-four out of ninety-three

patients (47.3%) had diffusive globular appearance (stage 2), which suggested that diffusive globular appearance is most common type of ducts dilation in SS patients. This result is consistent with Tonami's report [13].

Our results showed disagreement between fat signal staging and parotid duct dilation staging. This disagreement suggested that the pathological progressions in the parotid parenchyma and duct system are not developed in parallel. It also indicated that a comprehensive evaluation of parotid gland in SS patients requires both MR sialography and MRI imaging (T1WI, T2WI and STIR). Such combination of these two MR techniques will complement each other; facilitate diagnosis, treatment and prognosis of SS patients.

In summary, T2-3D-DRIVE MR sialography is capable of depicting the subtle changes that take place in the parotid gland ducts of patients with SS; while MRI imaging is capable of detecting the diffusive fat deposit in parotid gland. Two MR techniques, when combined, can most effectively diagnose SS; and serve as a valuable supplementary tool for the traditional X-ray sialography examine.

Disclosure of conflict of interest

None.

Address correspondence to: Li-Ling Long or Wei-Xiong Li, First Affiliated Hospital of Guangxi Medical University, 6 Shuangyong Road, Nanning, Guangxi 530021, China. E-mail: longlilingno1@163.com; cjr.longliling@vip.163.com (LLL); liwx668@sina.com (WXL)

References

[1] Patel RR, Carlos RC, Midia M and Mukherji SK. Apparent diffusion coefficient mapping of the normal parotid gland and parotid involvement in patients with systemic connective tissue disorders. AJNR Am J Neuroradiol 2004; 25: 16-20.

[2] Niemela RK, Takalo R, Paakko E, Suramo I, Paivansalo M, Salo T and Hakala M. Ultrasonography of salivary glands in primary Sjogren's syndrome. A comparison with magnetic resonance imaging and magnetic resonance sialography of parotid glands. Rheumatology (Oxford) 2004; 43: 875-879.

[3] Izumi M, Eguchi K, Ohki M, Uetani M, Hayashi K, Kita M, Nagataki S and Nakamura T. MR imaging of the parotid gland in Sjogren's syndrome: a proposal for new diagnostic criteria. AJR Am J Roentgenol 1996; 166: 1483-1487.

[4] Izumi M, Eguchi K, Nakamura H, Nagataki S and Nakamura T. Premature fat deposition in the salivary glands associated with Sjogren syndrome: MR and CT evidence. AJNR Am J Neuroradiol 1997; 18: 951-958.

[5] Ries T, Arndt C, Regier M, Graessner J, Cramer MC, Reitmeier F, Jaehne M, Adam G and Habermann CR. Value of apparent diffusion coefficient calculation before and after gustatory stimulation in the diagnosis of acute or chronic parotitis. Eur Radiol 2008; 18: 2251-2257.

[6] Regier M, Ries T, Arndt C, Cramer MC, Graessner J, Reitmeier F, Jaehne M, Adam G and Habermann CR. Sjögren's syndrome of the parotid gland: value of diffusion-weighted echo-planar MRI for diagnosis at an early stage based on MR sialography grading in comparison with healthy volunteers. Rofo 2009; 181: 242-248.

[7] Eida S, Sumi M, Sakihama N, Takahashi H and Nakamura T. Apparent diffusion coefficient mapping of salivary gland tumors: prediction of the benignancy and malignancy. AJNR Am J Neuroradiol 2007; 28: 116-121.

[8] Dirix P, De Keyzer F, Vandecaveye V, Stroobants S, Hermans R and Nuyts S. Diffusion-weighted magnetic resonance imaging to evaluate major salivary gland function before and after radiotherapy. Int J Radiat Oncol Biol Phys 2008; 71: 1365-1371.

[9] Ohbayashi N, Yamada I, Yoshino N and Sasaki T. Sjögren syndrome: comparison of assessments with MR sialography and conventional sialography. Radiology 1998; 209: 683-688.

[10] Vogl TJ, Dresel SH, Grevers G, Spath M, Bergman C, Balzer J and Lissner J. Sjoegren's syndrome: MR imaging of the parotid gland. Eur Radiol 1996; 6: 46-51.

[11] Makula E, Pokorny G, Kiss M, Voros E, Kovacs L, Kovacs A, Csernay L and Palko A. The place of magnetic resonance and ultrasonographic examinations of the parotid gland in the diagnosis and follow-up of primary Sjögren's syndrome. Rheumatology (Oxford) 2000; 39: 97-104.

[12] Fischbach R, Kugel H, Ernst S, Schroder U, Brochhagen HG, Jungehulsing M and Heindel W.

MR sialography: initial experience using a T2-weighted fast SE sequence. J Comput Assist Tomogr 1997; 21: 826-830.

[13] Tonami H, Ogawa Y, Matoba M, Kuginuki Y, Yokota H, Higashi K, Okimura T, Yamamoto I and Sugai S. MR sialography in patients with Sjogren syndrome. AJNR Am J Neuroradiol 1998; 19: 1199-1203.

[14] Gadodia A, Seith A, Sharma R, Thakar A and Parshad R. Magnetic resonance sialography using CISS and HASTE sequences in inflammatory salivary gland diseases: comparison with digital sialography. Acta Radiologica 2010; 51: 156-163.

[15] Valesini G, Gualdi GF, Priori R, Di Biasi C, Polettini E, Trasimeni G, Filippi A, Pivetti Pezzi P and Balsano F. Magnetic resonance imaging of the parotid glands and lip biopsy in the evaluation of xerostomia in Sjogren's syndrome. Scand J Rheumatol 1994; 23: 103-106.

[16] Spath M, Kruger K, Dresel S, Grevers G, Vogl T and Schattenkirchner M. Magnetic resonance imaging of the parotid gland in patients with Sjogren's syndrome. J Rheumatol 1991; 18: 1372-1378.

[17] Sartoretti-Schefer S, Kollias S, Wichmann W and Valavanis A. 3D T2-weighted fast spin-echo MRI sialography of the parotid gland. Neuroradiology 1999; 41: 46-51.

[18] Astreinidou E, Roesink JM, Raaijmakers CP, Bartels LW, Witkamp TD, Lagendijk JJ and Terhaard CH. 3D MR sialography as a tool to investigate radiation-induced xerostomia: feasibility study. Int J Radiat Oncol Biol Phys 2007; 68: 1310-1319.

[19] Vitali C, Bombardieri S, Jonsson R, Moutsopoulos HM, Alexander EL, Carsons SE, Daniels TE, Fox PC, Fox RI, Kassan SS, Pillemer SR, Talal N and Weisman MH. Classification criteria for Sjogren's syndrome: a revised version of the European criteria proposed by the American-European Consensus Group. Ann Rheum Dis 2002; 61: 554-558.

[20] Lomas DJ, Carroll NR, Johnson G, Antoun NM and Freer CE. MR sialography. Work in progress. Radiology 1996; 200: 129-133.

[21] Ciftci E, Anik Y, Arslan A, Akansel G, Sarisoy T and Demirci A. Driven equilibrium (drive) MR imaging of the cranial nerves V-VIII: comparison with the T2-weighted 3D TSE sequence. Eur J Radiol 2004; 51: 234-240.

[22] Niemela RK, Paakko E, Suramo I, Takalo R and Hakala M. Magnetic resonance imaging and magnetic resonance sialography of parotid glands in primary Sjogren's syndrome. Arthritis Rheum 2001; 45: 512-518.

[23] Tomiita M, Ueda T, Nagata H, Tanabe E, Shimojo N, Saito K, Motoori K, Ito H and Kohno Y. Usefulness of magnetic resonance sialography in patients with juvenile Sjogren's syndrome. Clin Exp Rheumatol 2005; 23: 540-544.